Available online at www.sciencedirect.com
SCIENCE DIRECT®
Biochemical Pharmacology 67 (2004) 1789–1799
Biochemical Pharmacology
www.elsevier.com/locate/biochempharm

Functional characterisation of the human α1 glycine receptor in a fluorescence-based membrane potential assay

Anders A. Jensen[a,*], Uffe Kristiansen[b]

[a]Department of Medicinal Chemistry, The Danish University of Pharmaceutical Sciences, Universitetsparken 2, Copenhagen DK-2100, Denmark
[b]Department of Pharmacology, The Danish University of Pharmaceutical Sciences, Universitetsparken 2, Copenhagen DK-2100, Denmark

Received 8 October 2003; accepted 22 December 2003

Abstract

In the present study, we have created a stable HEK293 cell line expressing the human homomeric α1 glycine receptor (GlyR) and characterised its functional pharmacology in a conventional patch-clamp assay and in the FLIPR® Membrane Potential (FMP) assay, a fluorescence-based high throughput screening assay. In the patch-clamp assay, the α1 GlyR exhibited the properties expected from a strychnine-sensitive glycine-gated chloride channel. In the FMP assay exposure of the cell line to GlyR agonists elicited a concentration-dependent increase in fluorescent intensity, a signal that could be suppressed by pre-incubation with GlyR antagonists. Agonists and antagonists displayed EC_{50} and K_i values in good agreement with previously reported values from studies of recombinant α1 GlyRs and native α1β GlyRs. The rank orders of potencies was glycine > β-alanine > taurine for the agonists and RU 5135 > strychnine > brucine > PMBA = picrotoxin > atropine for the antagonists. The actions of three allosteric modulators at the α1 GlyR cell line were also characterised in the FMP assay. Micromolar concentrations of Zn^{2+} inhibited α1 GlyR signalling but in contrast to previous reports the metal ion did not appear to potentiate GlyR function at lower concentrations. Analogously, whereas pregnenolone sulphate inhibited α1 GlyR function, the potentiation of α1 GlyR by pregnenolone in electrophysiological studies could not be reproduced in the assay. In conclusion, the FMP assay may not be suited for sophisticated studies of GlyR pharmacology and kinetics. However, the assay offers several advantages in studies of ligand–receptor interactions. Furthermore, the assay could be highly useful in the search for structurally novel ligands acting at GlyRs.

Keywords: Glycine receptor (GlyR); α1; FLIPR® Membrane Potential assay; NOVOstar™; High throughput screening (HTS); Fluorescence

1. Introduction

Inhibitory neurotransmission in the mammalian CNS is predominantly mediated by the amino acids γ-aminobutyric acid (GABA) and glycine. Glycinergic synapses are most abundant in spinal cord, brain stem and caudal brain, where the neurotransmitter is involved in the control of reflex responses, processing of sensory signals and motor rhythm generation [1–4]. Besides its role as a co-agonist at NMDA receptors [5], glycine exerts its effects via the strychnine-sensitive glycine receptors (GlyRs). These receptors belong to a superfamily of pentameric ligand-gated ion channels (LGICs), which also includes receptors for the neurotransmitters acetylcholine (ACh), GABA and serotonin and as well as a recently cloned Zn^{2+}-gated channel and invertebrate glutamate and histamine receptors [1–3]. The nicotinic ACh and serotonin 5-HT_3 receptors mediate excitatory transmission by the opening of cationic Na^+/Ca^{2+} channels and depolarisation of the postsynaptic cell, whereas activation of $GABA_{A/C}$Rs and GlyRs open anionic Cl^-/HCO_3^- channels leading to hyperpolarisation and inhibition of neuronal firing [1–4].

Abbreviations: ACh, acetylcholine; DMEM, Dulbecco's Modified Eagle Medium; FMP, FLIPR® Membrane Potential; GABA, γ-aminobutyric acid; GlyR, glycine receptor; HEK, human embryonic kidney; HTS, high throughput screening; nAChR, nicotinic ACh receptor; PMBA, ω-[2′-phosphonomethyl[1,1′-biphenyl]-3-yl]alanine; PREG, pregnenolone; PREGS, pregnenolone sulphate; RU 5135, 3α-hydroxy-16-imino-5β-17-azaandrostan-11-one

* Corresponding author. Tel.: +45-3530-6491; fax: +45-3530-6040.
E-mail address: aaj@dfuni.dk (A.A. Jensen).

0006-2952/$ – see front matter © 2004 Elsevier Inc. All rights reserved.
doi:10.1016/j.bcp.2003.12.037

To date five GlyR subunits have been cloned: four α subunits (α1–α4) and one β subunit. When expressed in *Xenopus* oocytes or in mammalian cell lines, functional GlyR complexes can be formed by the α subunits alone (homomeric GlyRs) or by α subunits together with the β subunit (heteromeric GlyRs). The composition of the native GlyRs changes during development. Embryonic GlyRs are predominantly α2 homomeric receptors, whereas the adult GlyR is composed by α1 and β subunits in a 3:2 stoichiometry [3,6,7].

The pharmacology of the homomeric α GlyR is very similar to that of the corresponding α/β heteromer, the major differences being that the homomeric GlyRs exhibit larger single channel conductances and are more sensitive to the antagonist picrotoxin than the corresponding heteromeric receptors [2,3,8]. Since the homomeric α1 GlyR displays functional properties similar to the adult native GlyR, it has become the prototypic recombinant GlyR subtype in electrophysiological and mutagenesis studies [2,3,8]. In the present study, we have created a stable HEK293 cell line expressing the human α1 GlyR and characterised its functional pharmacology in a conventional patch-clamp assay and in a fluorescence-based high throughput screening (HTS) assay.

2. Materials and methods

2.1. Materials

Culture media, serum, antibiotics and buffers for cell culture were obtained from Invitrogen (Paisley, Scotland). Glycine, taurine, β-alanine, (−)-strychnine (hereafter strychnine), brucine, ω-[2′-phosphonomethyl[1,1′-biphenyl]-3-yl]alanine (PMBA), atropine, pregnenolone (PREG) and pregnenolone sulphate (PREGS) were obtained from Sigma, and picrotoxin was purchased from Tocris Cookson. RU 5135 (3α-hydroxy-16-imino-5β-17-azaandrostan-11-one) was a kind gift from Dr. Mogens Nielsen (The Danish University of Pharmaceutical Sciences, Copenhagen, Denmark). The chemical structures of the compounds are given in Fig. 1. The cDNA for the human α1 GlyR subunit (α1-pIRES-EGFP) was a kind gift from professor Peter R. Schofield (Garvan Institute of Medical Research, Sydney, New South Wales, Australia).

2.2. Cell culture and generation of the stable cell line

The α1 GlyR subunit was subcloned from its original pIRES-EGFP vector into pCDNA3.1 using *Eco*RI as restriction enzyme. For the stable expression, HEK293 cells were maintained at 37 °C in a humidified 5% CO_2 incubator in culture medium (Dulbecco's Modified Eagle Medium (DMEM) supplemented with penicillin (100 U/ml), streptomycin (100 μg/ml) and 10% dialysed fetal bovine serum). The cells were transfected with α1-pCDNA3.1 using Polyfect as a DNA carrier according to the protocol by the manufacturer (Qiagen). The transfected cells were maintained for 2–3 weeks in selection medium containing 3 mg/ml G-418 and 10 μM strychnine. Antibiotic-resistant colonies were isolated and maintained in culture medium supplemented with 1 mg/ml G-418 and 10 μM strychnine for 3–4 weeks. Cell colonies were screened for a functional response to 1 mM glycine in the FMP assay (see below). In this screening, several cell clones exhibiting a significant response to glycine exposure were identified, and one of these were selected for further characterisation in the patch-clamp assay and the FMP assay.

2.3. Electrophysiological recordings

The α1 GlyR-HEK293 cells were split into poly-D-lysine-coated 35 mm Petri dishes in culture medium supplemented with 1 mg/ml G-418. 16–24 h later the culture medium was exchanged for an extracellular recording solution containing (in mM): NaCl 140, KCl 3.5, Na_2HPO_4 1.25, $MgSO_4$ 2, $CaCl_2$ 2, glucose 10, and HEPES 10; pH 7.35. The Petri dish with cells was transferred to the stage of an inverted phase-contrast Axiovert 10 microscope (Zeiss). The cells were constantly perfused with extracellular recording solution (0.5 ml/min) at room temperature from a gravity fed 7-barrelled perfusion pipette (List, Germany) approximately 100 μm from the recorded neuron. By switching application from one barrel to another, the extracellular solution surrounding the neuron was exchanged with a time constant of ∼50 ms. Individual cells were approached with micropipettes of 2–3 MΩ resistance manufactured from 1.5 mm o.d. glass (World Precision Instruments). The intrapipette solution contained (in mM): KCl 140, $MgCl_2$ 1, $CaCl_2$ 1, EGTA 10, MgATP 2, and HEPES 10; pH 7.3. Standard patch-clamp techniques [9] in voltage clamp mode were used to record from neurons in the whole-cell configuration using an EPC-9 amplifier (HEKA Elektronik). Clamping potentials were corrected for liquid junction potentials. Series resistance was 70–80% compensated. The high intracellular Cl^- concentration shifted the Cl^- reversal potential to approximately 0 mV and substantially increased the currents recorded at −64 mV. Whole-cell membrane currents were plotted on a low fidelity chart recorder during the experiment and stored on computer hard disk and videotape using a VR-10B digital data recorder (Instrutech).

Glycine and strychnine were dissolved in distilled water at a concentrations at least 100× greater than that required for perfusion and diluted with extracellular recording solution. Different concentrations of glycine were applied for 5 s at 1 min intervals. Strychnine was preapplied for 10 s immediately before application of a premixed solution of glycine and solution.

Membrane currents were analysed using Pulse (HEKA Elektronik) software. Currents were normalised to the peak current induced by 3 mM glycine in the same cell.

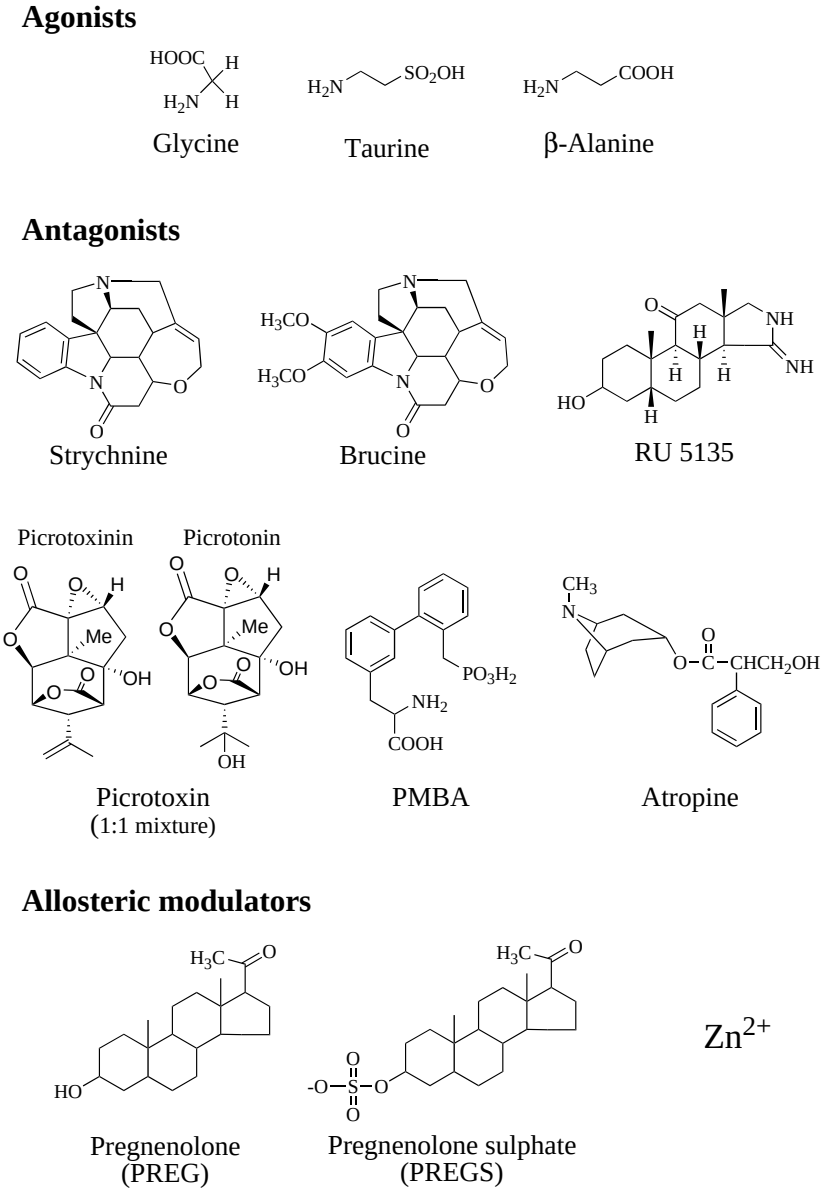

Fig. 1. Chemical structures of the compounds characterised at the α1 GlyR-HEK293 cell line.

Concentration–response relationships were fitted to the equation:

$$I = \frac{I_{max}}{(1 + (EC_{50}/[glycine])^n)}$$

where I is the membrane current induced by a glycine concentration [glycine], I_{max} is the maximum current that glycine can induce, EC_{50} is the glycine concentration eliciting 50% of I_{max}, and n is the Hill coefficient. Data were described using mean and standard error (S.E.) or 95% confidence intervals.

2.4. The FLIPR® Membrane Potential (FMP) assay

The pharmacology of the α1 GlyR-HEK293 cell line was characterised in the FMP assay according to the protocol of the manufacturer (Molecular Devices). The lipophilic, anionic, bis-oxonol dye in this kit is excited at 530 nm, and the distribution of the dye across the plasma membrane is dependent on the membrane potential of the cell. Hence, depolarisation of the cells will cause more dye to enter the cells, where it will bind to intracellular proteins and lipids and cause an increase in the fluorescence signal. Conversely, the dye exits the cells upon hyperpolarisation giving rise to a decrease in the fluorescence signal.

The α1 GlyR-HEK293 cells were split into poly-D-lysine-coated black 96-well plates (Packard) in culture medium supplemented with 1 mg/ml G-418. 16–24 h later the medium was aspirated, and washed with 100 μl Krebs buffer (140 mM NaCl/4.7 mM KCl/2.5 mM $CaCl_2$/1.2 mM $MgCl_2$/11 mM HEPES/10 mM D-glucose, pH 7.4). Fifty microlitres Krebs buffer was added to each well (in the antagonist experiments, various concentrations of the antagonists were dissolved in the buffer). Fifty microlitres

of loading buffer (loading dye dissolved in Krebs buffer) was added to each well, and the plate was incubated at 37 °C in a humidified 5% CO_2 incubator for 30 min. The plate was assayed in a NOVOstar™ plate reader (BMG Labtechnologies) measuring emission (in fluorescence units (FU)) at 560 nm caused by excitation at 530 nm before and up to 1 min after addition of 25 μl agonist solution (agonist was dissolved in Krebs buffer). The experiments were performed in duplicate at least three times for each compound. The detailed characterisation of the interactions of antagonists strychnine, RU 5135 and PMBA and allosteric modulators Zn^{2+}, PREG and PREGS with α1 GlyR were performed exactly according to the protocol described above.

2.5. Data analysis

Concentration–response curves for agonists and antagonists were constructed based on the maximal responses at different concentrations of the respective ligands. The curves were generated by nonweighted least-squares fits using the program KaleidaGraph 3.6 (Synergy Software). Antagonist potencies were calculated from the inhibition curves using the ''functional equivalent'' of the Cheng–Prusoff equation $K_i = IC_{50}/[1 + ([A]/EC_{50})]$ [10], where [A] is the agonist concentration used in the specific experiment.

3. Results

In a conventional patch-clamp set-up the stable α1 GlyR-HEK293 cell line displayed the characteristics of a strychnine-sensitive glycine-gated Cl^- channel (Fig. 2). When cells were voltage-clamped at −64 mV application of glycine gave rise to a concentration-dependent inward current, which at the lowest concentration (10 μM) reached a stable plateau but at the higher concentrations rose quickly to a peak and faded within the 5 s of glycine application. Analysis of the concentration–response relationship of the peak currents revealed an EC_{50} of 91 μM (95% confidence interval [77; 108]) and a Hill coefficient of 2.0 (95% confidence interval [1.3; 2.8]). We also analysed the currents remaining after 5 s of agonist application. This resulted in an EC_{50} of 56 μM (95% confidence interval [31; 103]) and Hill coefficient 2.3 (95% confidence interval [1.0; 3.6]) (Fig. 2A). These parameters were not significantly different from those calculated from the peak currents. The wider confidence intervals of the EC_{50} and the Hill coefficient for the currents remaining after 5 s are probably due to the lack of points on the steep part of the corresponding concentration–response curve. The voltage dependence of the glycine-gated current was investigated using 100 μM glycine and clamping potentials ranging from −64 to +36 mV (Fig. 2B). The current–voltage relationship showed modest outward rectification and a reversal potential close to 0 mV, as expected with nearly equal Cl^- concentrations on each side of the cell membrane. Based on the reversal potentials of the individual cells a mean value of 1.75 ± 0.3 mV was calculated. Assuming an intracellular Cl^- concentration equal to the

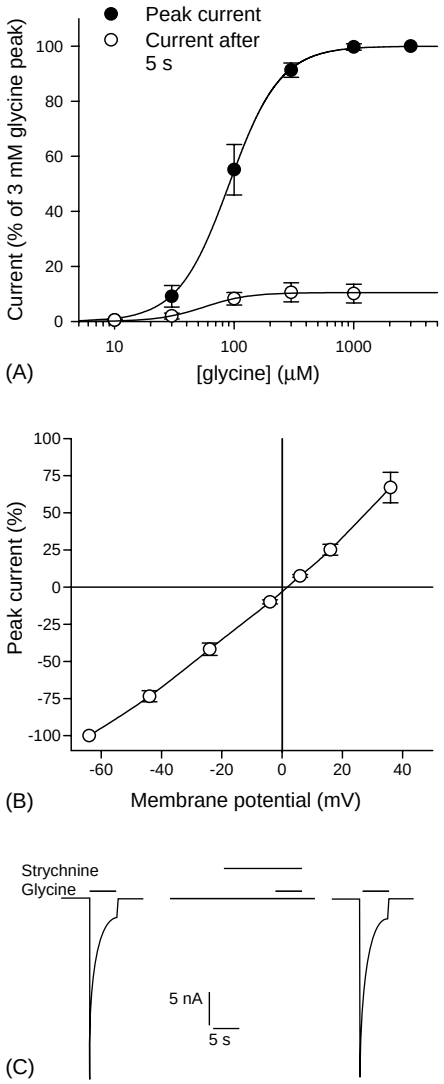

Fig. 2. Pharmacological characterisation of the α1 GlyR-HEK293 cell line in the patch-clamp set-up. The experimental procedures used are described in Section 2. (A) Concentration–response relationship for glycine induced peak currents (closed circles) and currents remaining after 5 s of glycine application (open circles) at a holding potential of −64 mV. Currents were normalised to the peak current induced by 3 mM glycine in each cell and shown as mean ± S.E.M. ($n = 7$). Non-linear regression analysis (solid curves) showed $EC_{50} = 91$ μM (95% confidence interval [77; 108]) and Hill coefficient = 2.0 (95% confidence interval [1.3; 2.8]) for the peak currents while for the currents remaining after 5 s of agonist application EC_{50} was 56 μM (95% confidence interval [31; 103]) and the Hill coefficient 2.3 (95% confidence interval [1.0; 3.6]). (B) Current–voltage relationship for peak membrane currents induced by 100 μM glycine. Currents were normalized to the peak current induced at −64 mV in each cell (−100%) and shown as mean ± S.E.M. ($n = 6$). (C) Example of the effect of 10 μM strychnine on the current induced by 1 mM glycine. Horizontal bars above the current traces indicate application of the two drugs. When 10 μM strychnine was co-applied with glycine the current was reduced to 0.007 ± 0.007% (mean ± S.E.M., $n = 7$) of the control value.

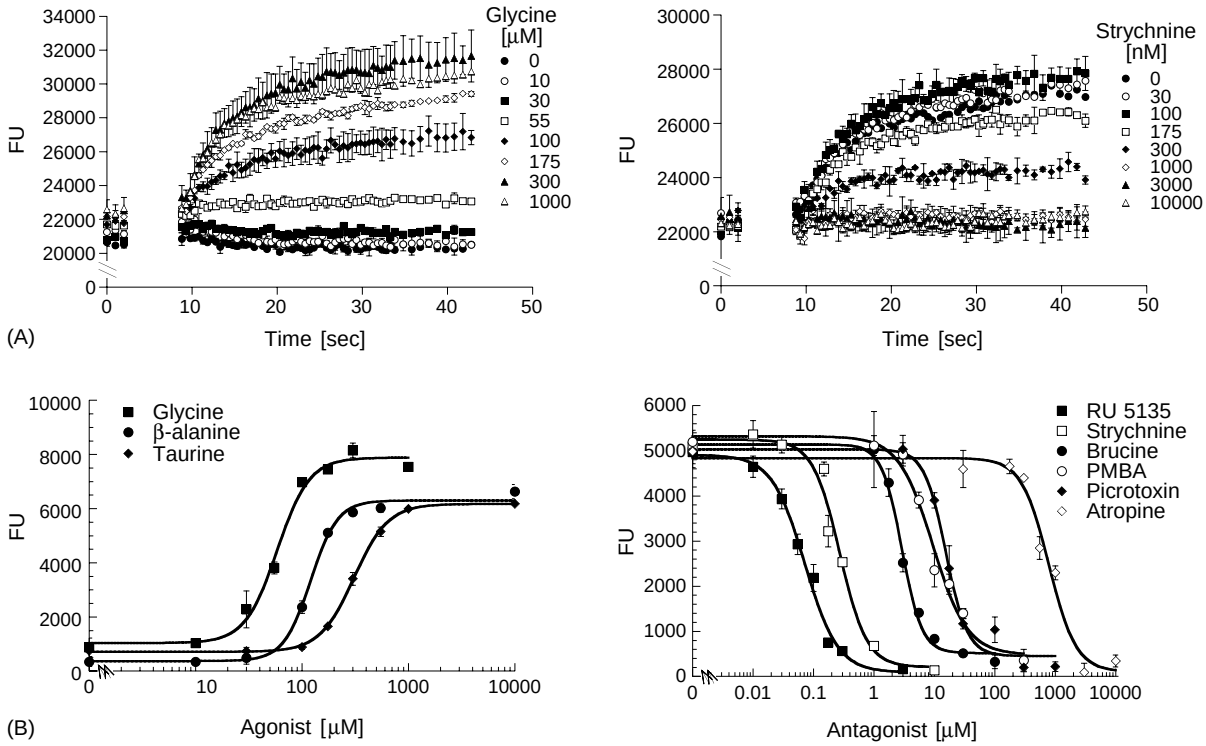

Fig. 3. Agonist and antagonist pharmacology of α1 GlyR in the FMP assay. (A) Time–response curves for the glycine-induced response in the α1 GlyR-HEK293 cell line and the antagonism exerted by strychnine. Measurement of fluorescence (FU) was performed immediately before (seconds 0–3) and after (seconds 8–42) addition of glycine to the wells and mixture of the final solution. (B) Concentration–response curves of agonists and antagonists at the α1 GlyR-HEK293 cell line. The experimental procedures are described in Section 2. In the antagonist experiments, 100 μM glycine was used as agonist. The graphs in (A) and (B) are based on individual experiments.

intrapipette concentration a theoretical Cl^- equilibrium potential of −0.6 mV was calculated from the Nernst equation. The sensitivity of glycine-gated currents to the GlyR antagonist strychnine was investigated using 1 mM glycine. When 10 μM strychnine was co-applied with glycine the current was reduced to $0.007 \pm 0.007\%$ (mean ± S.E.M., $n = 7$) of the control value (Fig. 2C).

In the FMP assay, exposure of the α1 GlyR-HEK293 cell line to GlyR agonists gave rise to solid concentration-dependent increases in fluorescent intensity (exemplified by glycine in Fig. 3A). This response could be suppressed in a concentration-dependent manner by pre-incubation of antagonist (exemplified by strychnine in Fig. 3A). In order to characterise the pharmacology of the α1 GlyR-HEK293 cell line in the assay in detail, the functional properties of three agonists, six structurally diverse antagonists and three allosteric modulators were determined in this manner (Fig. 1).

The endogenous GlyR agonists glycine, taurine and β-alanine displayed EC_{50} values in the high micromolar range and Hill slopes between 2 and 3 (Fig. 3B and Table 1). Since exposure of non-transfected HEK293 cells to the three agonists in 10 mM concentrations did not give rise to any significant fluorescent response, the agonist-induced signal in the stable cell line was clearly mediated by α1 GlyR (data not shown). The GlyR antagonists strychnine, brucine, picrotoxin, PMBA, RU 5135 and atropine all inhibited the glycine-induced response through the receptor in a concentration-dependent manner (Fig. 3B and Table 1). The pharmacological data for both agonists and antagonists were highly reproducible.

The pharmacological profiles of three of the antagonists strychnine, RU 5135 and PMBA were characterised in greater detail. Concentration–response relationships for the antagonists at five different glycine concentrations and concentration–response relationships for glycine in the absence and presence of various antagonist concentrations are depicted in Fig. 4. The IC_{50} values for all three antagonists increased with increasing glycine concentrations, whereas their calculated K_i values were not significantly different in the different experiments (Fig. 4, upper panel). Furthermore, the potency of glycine at the α1 GlyR was decreased in the presence of increasing concentrations of the antagonists, whereas the maximal response of the agonist was not influenced by the different antagonist concentrations used (Fig. 4, lower panel).

Zn^{2+} and the neurosteroids PREG and PREGS have been reported to be allosteric modulators of GlyR function [11–17]. In the FMP assay, Zn^{2+} and PREGS inhibited α1 GlyR function with IC_{50} values in the mid-micromolar range (Fig. 5A and B and Table 1). The antagonism of both allosteric modulators appeared to be predominantly competitive in nature, since the EC_{50} value of glycine was increased in the presence of increasing concentrations of

Table 1
Pharmacological characteristics of the α1 GlyR-HEK293 cell line in the FMP assay

Compound	FMP assay			Electrophysiology (*Xenopus* oocytes or HEK293 cells)	
	EC_{50} (μM) (pEC_{50} ± S.E.M.)	n_H	*n*	EC_{50} (μM)	n_H
Agonists					
Glycine	82 (4.08 ± 0.07)	2.6 ± 0.23	8	25[a], 25–280[b], 158[c], 25[d], 290[e], 18[f], 18[h]	1.7[a], 1.7-3[b], 1.8[d], 1.7[h]
Taurine	490 (3.31 ± 0.12)	2.7 ± 0.12	3	178[a], 167–3400[b], 153[f], 920[g]	2.5[a], 1.2-3[b], 1.7[g]
β-Alanine	180 (3.75 ± 0.08)	3.0 ± 0.27	5	48[a], 52[f]	2.2[a]
	K_i (μM) (pK_i ± S.E.M.)			K_i (μM)	
Antagonists					
Strychnine	0.11 (6.96 ± 0.09)		7	0.029[a], 0.016[e]	
Brucine	1.01 (5.99 ± 0.06)		4	–	
Picrotoxin	4.2 (5.38 ± 0.13)		4	3.1 (IC_{50} @ 30 μM glycine)[d] 25 (IC_{50} @ EC_{50} glycine)[h]	
PMBA	3.5 (5.46 ± 0.05)		5	0.406 (IC_{50} @ EC_{50} glycine)[i]	
RU 5135	0.021 (7.68 ± 0.11)		5	–	
Atropine	220 (3.66 ± 0.11)		3	161[j]	
	IC_{50} (μM) (pIC_{50} ± S.E.M.)			EC_{50}/IC_{50} (μM)	
Allosteric modulators					
Zn^{2+}	23 (4.63 ± 0.07)		5	Potentiation/inhibition (EC_{50} 0.85/IC_{50} 22)[k] Potentiation/inhibition (EC_{50} 0.08/IC_{50} 546)[l]	
PREGS	14 (4.85 ± 0.09)		5	Inhibition (IC_{50} 1.9)[c]	
PREG	N.E.		3	Potentiation (EC_{50} 1.4)[c]	

The experimental procedures used are described in Section 2. The IC_{50} values for the allosteric modulators were determined in the presence of 100 μM glycine. The pharmacological properties from selected studies of human α1 GlyR expressed in *Xenopus* oocytes or HEK293 cells and assayed by conventional electrophysiology are given for comparison. N.E., no effect.

[a] The electrophysiology data is from reference [25].
[b] The electrophysiology data is from reference [27].
[c] The electrophysiology data is from reference [11].
[d] The electrophysiology data is from reference [14].
[e] The electrophysiology data is from reference [26].
[f] The electrophysiology data is from reference [28].
[g] The electrophysiology data is from reference [16].
[h] The electrophysiology data is from reference [29].
[i] The electrophysiology data is from reference [31].
[j] The electrophysiology data is from reference [39].
[k] The electrophysiology data is from reference [15].
[l] The electrophysiology data is from reference [17].

Zn^{2+} or PREGS (Fig. 5A and B, lower panel). In contrast, PREG in concentrations up to 100 μM had no significant effect on α1 GlyR signalling (Fig. 5C). In the experiments in Fig. 5, the allosteric modulators were applied to α1 GlyR 30 min prior to glycine exposure. However, when Zn^{2+}, PREGS or PREG were co-applied with glycine, their pharmacological profiles were not significantly different from those depicted in Fig. 5 (data not shown).

4. Discussion

In recent years fluorescence-based HTS assays have been applied extensively in the search for small molecule modulators of membrane-bound effector proteins such as voltage-gated ion channels, G-protein coupled receptors and the ligand-gated ion channels for glutamate, GABA and ACh [18–22]. This study represents the first pharmacological characterisation of a glycine receptor in one of these assays.

It is important to realise the differences underlying the pharmacological characteristics of the α1 GlyR determined in the patch-clamp assay and in the FMP assay. In the voltage-clamp experiment the membrane potential of the α1-HEK293 cell is clamped at a fixed value (Fig. 2). The increase in current measured during application of an agonist, which opens Cl^- channels, is therefore directly proportional to the number of open channels, assuming a homogeneous population of Cl^- channels with equal conductance. In the FMP assay, however, the change in membrane potential is not a linear function of the number of Cl^- channels opened by an agonist. Rather, as predicted by the Goldman equation, when the number of open channels increases, the membrane potential approaches asymptotically the equilibrium potential of Cl^- [23]. The change in membrane potential per channel opened is largest for the first channels and approaches zero as more and more channels open. Thus, when using membrane potential as response parameter, the relationship between agonist concentration and response will be distorted and, in

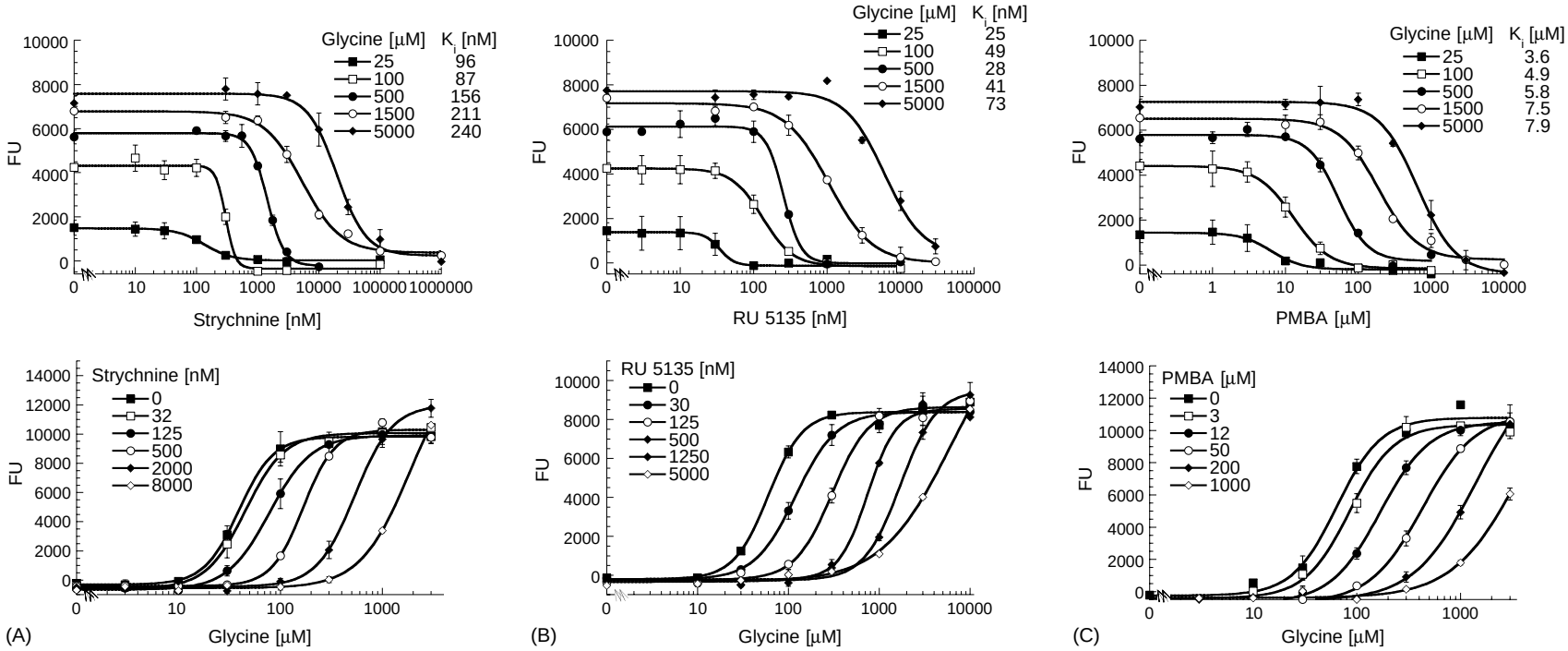

Fig. 4. Antagonist pharmacology of α1 GlyR in the FMP assay. Detailed analysis of the interactions of α1 GlyR with the antagonists strychnine (A), RU 5135 (B) and PMBA (C). In the upper panel, concentration–response relationships for the three antagonists at five different glycine concentrations are depicted. The calculated K_i values for the antagonists at the different agonist concentrations are indicated. In the lower panel, concentration–response relationships for glycine in the absence and in the presence of five different antagonist concentrations are depicted. The experimental procedures are described in Section 2.

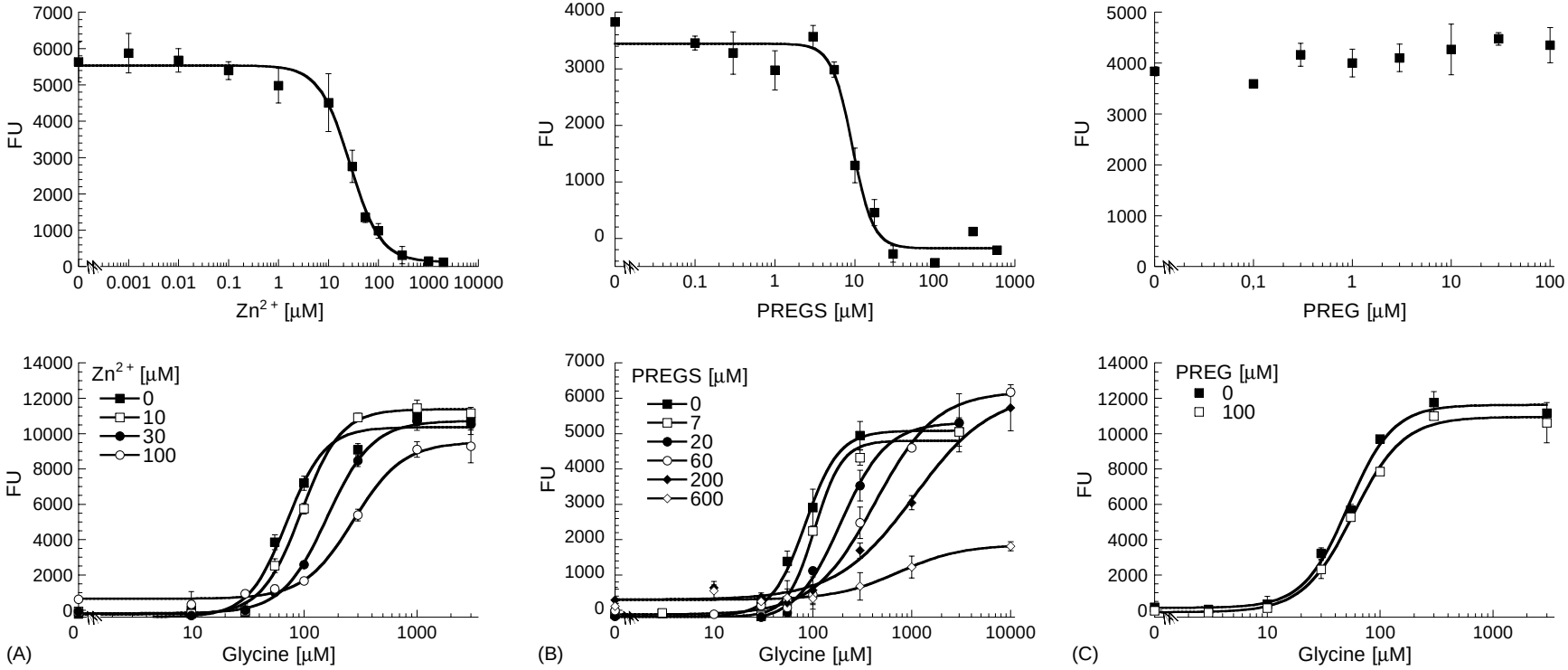

Fig. 5. Allosteric modulation of α1 GlyR in the FMP assay. The allosteric modulation of glycine-induced GlyR signalling exerted by Zn^{2+} (A), PREGS (B) and PREG (C). In the upper panel, concentration–response relationships for the allosteric modulators using 100 μM glycine as agonist concentration are depicted. In the lower panel, concentration–response relationships for glycine in the absence or presence of various concentrations of allosteric modulator are depicted. The experimental procedures are described in Section 2.

particular, the efficacies of partial agonists may be overestimated. Another potential source of discrepancy between results from the patch-clamp experiments and the membrane potential assay is the different timing of the response measurements. In the patch-clamp experiments, we have measured the peak responses, which are minimally influenced by desensitisation, and also the currents remaining after 5 s of agonist application, which are considerably but not fully desensitised (Fig. 2C). If agonist application was prolonged in order to reach steady-state desensitisation it would take several minutes before the receptors had recovered from desensitisation and the agonist could be applied again, which is not compatible with the limited duration of most whole-cell recordings.

In the membrane potential assay responses are measured later when a steady state has been reached and they are therefore more influenced by receptor desensitisation. Nevertheless, in the present study the EC_{50} values and Hill coefficients for glycine are in good agreement for the two methods (Fig. 2A and Table 1).

The observation that application of GlyR agonists to the α1-HEK293 cell line in the FMP assay gave rise to an increase in fluorescent intensity might seem surprising. According to the manufacturer of the FMP assay kit (Molecular Devices), an increase in the intensity of the fluorescence signal in this assay should reflect cell depolarisation, and this correlation has been demonstrated in studies of nAChRs in the FMP assay [21,22]. The extracellular Cl^- concentration used in this assay (≈150 mM) is similar to that in the patch-clamp assay. In a membrane potential assay, the change in membrane potential resulting from agonist-induced opening of Cl^- channels depends on the resting membrane potential as well as on the equilibrium potential of Cl^-, the latter being a function of the intracellular and extracellular Cl^- concentrations. In many mammalian cells, the Cl^- equilibrium is similar to or more negative than the resting membrane potential, and opening of Cl^- consequently leads to hyperpolarisation. However, in certain cell types, including some embryonic cells, opening of Cl^- channels results in depolarisation, most likely due to a relatively high intracellular Cl^- concentration [24]. In any case, considering that the α1 GlyR cell line displayed electrophysiological properties expected for a chloride channel and that the pharmacological characteristics for a wide range of structural diverse GlyR ligands in the FMP assay were in excellent agreement with previous studies of recombinant α1 GlyRs and native GlyRs, there is no doubt that the observed increase in fluorescent intensity upon agonist-exposure is a α1 GlyR-mediated event.

In the FMP assay, glycine exhibited an EC_{50} of 82 μM at α1 GlyR, with β-alanine and taurine displaying two- and sixfold lower potencies, respectively. The potencies and the rank order of the three agonists were in good agreement with electrophysiology studies of the human α1 GlyR expressed in mammalian cell lines or in *Xenopus* oocytes (Table 1) [25–28]. In the FMP assay the maximal responses of taurine and β-alanine were not significantly different from that of glycine (Fig. 3B). Although the efficacy of taurine at α1 GlyR has varied considerably in previous studies using mammalian cells or *Xenopus* oocytes, it is normally considered to be a partial agonist at the receptor [15,16,25,27,28]. In a recent study, we have found the FMP assay to be unable to discriminate between full and partial agonists at a α3β4 nAChR-HEK293 cell line, so it is valid to question whether the assay would be able to do so with the α1 GlyR [21]. An explanation for this inability could be the above-mentioned non-linear relationship between receptor activation and change in membrane potential.

In a study of various nAChR subtypes in the FMP assay, the K_i values for antagonists were found to be significantly higher than in conventional electrophysiology or patch-clamp systems [22]. However, this does not seem to be the case for the α1 GlyR-HEK293 cell line (Table 1). The antagonist potencies and the rank order of the six antagonists characterised at the cell line (RU 5135 > strychnine > brucine > PMBA = picrotoxin > atropine) were in good agreement with the findings from previous studies of the compounds on recombinant α1 or native α1β GlyRs. The classic antagonists picrotoxin and strychnine exhibited K_i values similar to and slightly (fivefold) higher, respectively, than those obtained in electrophysiological studies (Table 1) [25,26,29,30]. PMBA was 10-fold weaker as an antagonist in this study than in an electrophysiology study of α1 GlyR expressed in *Xenopus* oocytes (Table 1) [31]. On the other hand, PMBA has also been reported to inhibit native GlyRs with a potency in the midmicromolar range [32]. To our knowledge the strychnine analogue brucine and the steroid derivative RU 5135 have not previously been characterised at recombinant GlyRs. However, the functional antagonism displayed by the two compounds at the α1 GlyR-HEK293 cell line correlated nicely with binding data. RU 5135 has displayed low nanomolar binding affinities at native rat GlyRs, and the steroid derivative has been estimated to be 10- to 15-fold more potent than strychnine [33–35]. Brucine, on the other hand, has displayed 15- to 20-fold lower binding affinities than strychnine to native rat and pigeon GlyRs [36,37]. In the FMP assay, RU 5135 and brucine displayed fivefold higher and ninefold lower antagonistic potency than strychnine, respectively (Table 1). In agreement with previous studies, atropine was found to be a weak antagonist of α1 GlyR (Table 1) [38,39].

Taking advantage of the prolific nature of the FMP assay, we characterised the antagonism of strychnine, PMBA and RU 5135 in some detail (Fig. 4). It is well-documented that the binding site of strychnine in the GlyR overlaps the agonist binding site [2,3], and PMBA and RU 5135 have also been shown to displace [^{3}H]strychnine binding and inhibit glycine-induced responses through native GlyRs in a competitively manner [32,33,35]. The K_i values determined for the three compounds at five different glycine concentrations in the FMP assay were very similar,

although the antagonistic potencies of strychnine and PMBA seemed to decrease slightly with higher agonist concentrations (Fig. 4). Furthermore, the potency of glycine decreased with increasing concentrations of antagonists, whereas the maximal responses exhibited by the agonist were unchanged. All in all, the three compounds must be said to display antagonistic profiles in the FMP assay characterised by a predominant competitive component (Fig. 4).

The GlyRs are subjected to allosteric modulation by a wide range of structurally diverse ligands [2,3]. Zn^{2+} has been demonstrated to potentiate GlyR function at concentrations below 10 μM, whereas the metal ion inhibits the receptor at concentrations between 10 and 1000 μM [13–17]. The potentiation and inhibition by zinc are mediated through multiple distinct binding sites in the N-terminal domain of α1 GlyR [14–16]. Zn^{2+} binding to the site responsible for the potentiation has been proposed to cause a decreased dissociation rate of the agonist from the receptor and Zn^{2+} binding to the inhibitory site to impair the gating of the GlyR channel [16]. The presence of 10 μM Zn^{2+} has also been demonstrated to increase the potency and the maximal response of taurine at α1 GlyR, converting it from a partial agonist to a full agonist, whereas the metal ion inhibited the taurine signal at higher concentrations [16]. In the FMP assay, Zn^{2+} inhibited the α1 GlyR signalling elicited by 100 μM glycine with an IC_{50} of 23 μM (Fig. 5A and Table 1). In contrast, we did not observe any significant potentiation of the receptor signalling at lower concentrations of the metal ion (Fig. 5A). Furthermore, neither EC_{50} nor the maximal response of taurine was increased in the presence of Zn^{2+} but the metal ion inhibited the α1 GlyR response elicited by 700 μM taurine in a concentration-dependent manner with an IC_{50} of 89 μM (data not shown).

PREG and its 3β-sulphate derivative PREGS are other allosteric GlyR modulators with distinct effects at different subtypes. PREG has been shown to potentiate α1 GlyR function, having no effect on the signalling of α2 and α1β GlyRs [11,12]. In contrast, PREGS inhibits signalling through all three GlyR subtypes [11]. In the FMP assay, α1 GlyR signalling was inhibited by midmicromolar concentration of PREGS, whereas no potentiation of receptor function was observed in the presence of PREG (Fig. 5B and C). The fact that neither potentiation of α1 GlyR by Zn^{2+} or PREG could be reproduced in the FMP assay could suggest that this assay is unable to detect allosteric potentiation of the receptor. Another explanation could be differences in the kinetics of the potentiation and inhibition processes. Schofield and co-workers have demonstrated that Zn^{2+} potentiation of α1 GlyR is characterised by a rapid onset and recovery, whereas the processes underlying the inhibition mediated by the metal ion are considerably slower [15]. Considering that no fluorescence recordings are being performed in the time frame from agonist addition to the end of assay solution mixture, a time period of 5.8 s (see Fig. 3A), the potentiation of α1 GlyR exerted by Zn^{2+}, and possibly also PREG, may not be detected in the FMP assay.

In conclusion, we have implemented a HTS assay suitable for the characterisation of GlyRs. While the assay is not suited for sophisticated and mechanistic studies of GlyR pharmacology and kinetics, the high reproducibility and the prolific nature of the assay allow for elaborate studies of GlyR pharmacology. Furthermore, the assay should accommodate pharmacological characterisation of GlyR combinations other than the α1 GlyR. In preliminary studies, a stable HEK293 cell line expressing the human heteromeric α1β GlyR has been found to be functional in the assay (data not shown). Finally, the ability to screen diverse compound libraries will be very useful in the search for structurally novel compounds targeted at various GlyR subtypes.

Acknowledgments

The authors wish to thank professor Peter R. Schofield and Dr. Mogens Nielsen for their generous gifts of the human α1 GlyR cDNA and the RU 5135 sample, respectively. Professor Hans Bräuner-Osborne is thanked for his critical review of the manuscript. This work was supported by the Augustinus Foundation, the Director Ib Henriksen Foundation, the Lundbeck Foundation (A.A.J.) and the Danish MRC (#22-01-0291) (U.K.).

References

[1] Breitinger HG, Becker CM. The inhibitory glycine receptor: prospects for a therapeutic orphan? Curr Pharm Des 1998;4:315–34.
[2] Laube B, Maksay G, Schemm R, Betz H. Modulation of glycine receptor function: a novel approach for therapeutic intervention at inhibitory synapses? Trends Pharmacol Sci 2002;23:519–27.
[3] Rajendra S, Lynch JW, Schofield PR. The glycine receptor. Pharmacol Ther 1997;73:121–46.
[4] Moss SJ, Smart TG. Constructing inhibitory synapses. Nat Rev Neurosci 2001;2:240–50.
[5] Dingledine R, Borges K, Bowie D, Traynelis SF. The glutamate receptor ion channels. Pharmacol Rev 1999;51:7–61.
[6] Langosch D, Thomas L, Betz H. Conserved quaternary structure of ligand-gated ion channels: the postsynaptic glycine receptor is a pentamer. Proc Natl Acad Sci USA 1988;85:7394–8.
[7] Takahashi T, Momiyama A, Hirai K, Hishinuma F, Akagi H. Functional correlation of fetal and adult forms of glycine receptors with developmental changes in inhibitory synaptic receptor channels. Neuron 1992;9:1155–61.
[8] Betz H, Kuhse J, Schmieden V, Laube B, Kirsch J, Harvey RJ. Structure and functions of inhibitory and excitatory glycine receptors. Ann NY Acad Sci 1999;868:667–76.
[9] Hamill OP, Marty A, Sakmann B, Sigworth FJ. Improved patchclamp techniques for high-resolution current recording from cells and cell-free membrane patches. Pfluegers Arch 1981;391:85–100.
[10] Craig DA. The Cheng–Prusoff relationship: something lost in the translation. Trends Pharmacol Sci 1993;14:89–91.
[11] Maksay G, Laube B, Betz H. Subunit-specific modulation of glycine receptors by neurosteroids. Neuropharmacology 2001;41:369–76.

[12] Wu FS, Chen SC, Tsai JJ. Competitive inhibition of the glycine-induced current by pregnenolone sulfate in cultured chick spinal cord neurons. Brain Res 1997;750:318–20.
[13] Bloomenthal AB, Goldwater E, Pritchett DB, Harrison NL. Biphasic modulation of the strychnine-sensitive glycine receptor by Zn^{2+}. Mol Pharmacol 1994;46:1156–9.
[14] Laube B, Kuhse J, Rundstrom N, Kirsch J, Schmieden V, Betz H. Modulation by zinc ions of native rat and recombinant human inhibitory glycine receptors. J Physiol 1995;83:613–9.
[15] Lynch JW, Jacques P, Pierce KD, Schofield PR. Zinc potentiation of the glycine receptor chloride channel is mediated by allosteric pathways. J Neurochem 1998;71:2159–68.
[16] Laube B, Kuhse J, Betz H. Kinetic and mutational analysis of Zn^{2+} modulation of recombinant human inhibitory glycine receptors. J Physiol 2000;522:215–30.
[17] Harvey RJ, Thomas P, James CH, Wilderspin A, Smart TG. Identification of an inhibitory Zn^{2+} binding site on the human glycine receptor α1 subunit. J Physiol 1999;520:53–64.
[18] Varney MA, Rao SP, Jachec C, Deal C, Hess SD, Daggett LP, et al. Pharmacological characterization of the human ionotropic glutamate receptor subtype GluR3 stably expressed in mammalian cells. J Pharmacol Exp Ther 1998;285:358–70.
[19] Grobin AC, Inglefield JR, Schwartz-Bloom RD, Devaud LL, Morrow AL. Fluorescence imaging of $GABA_A$ receptor-mediated intracellular $[Cl^-]$ in P19-N cells reveal unique pharmacological properties. Brain Res 1999;827:1–11.
[20] Adkins CE, Pillai GV, Kerby J, Bonnert TP, Haldon C, McKernan RM, et al. α4β3δ $GABA_A$ receptors characterized by fluorescence resonance energy transfer-derived measurements of membrane potential. J Biol Chem 2001;276:38934–9.
[21] Jensen AA, Mikkelsen I, Frølund B, Bräuner-Osborne H, Falch E, Krogsgaard-Larsen P. Carbamoylcholine homologs: novel and potent agonists at neuronal nicotinic acetylcholine receptors. Mol Pharmacol 2003;64:865–75.
[22] Fitch RW, Xiao Y, Kellar KJ, Daly JW. Membrane potential fluorescence: a rapid and highly sensitive assay for nicotinic receptor channel function. Proc Natl Acad Sci USA 2003;100:4909–14.
[23] Koester J. Membrane potential. In: Kandel ER, Schwartz JH, Jessel TM, editors. Principles of neuroscience. New York: Elsevier; 1991.
[24] Serafini R, Valeyev AY, Barker JL, Poulter MO. Depolarizing GABA-activated Cl^- channels in embryonic rat spinal and olfactory bulb cells. J Physiol 1995;488:371–86.
[25] Vafa B, Lewis TM, Cunningham AM, Jacques P, Lynch JW, Schofield PR. Identification of a new ligand binding domain in the α1 subunit of the inhibitory glycine receptor. J Neurochem 1999;73:2158–66.
[26] Grenningloh G, Schmieden V, Schofield PR, Seeburg PH, Siddique T, Mohandas TK, et al. Alpha subunit variants of the human glycine receptor: primary structures, functional expression and chromosomal localization of the corresponding genes. EMBO J 1990;9:771–6.
[27] De Saint Jan D, David-Watine B, Korn H, Bregestovski P. Activation of human α1 and α2 homomeric glycine receptors by taurine and GABA. J Physiol 2001;535:741–55.
[28] Lynch JW, Rajendra S, Pierce KD, Handford CA, Barry PH, Schofield PR. Identification of intracellular and extracellular domains mediating signal transduction in the inhibitory glycine receptor chloride channel. EMBO J 1997;16:110–20.
[29] Handford CA, Lynch JW, Baker E, Webb GC, Ford JH, Sutherland GR, et al. The human glycine receptor beta subunit: primary structure, functional characterisation and chromosomal localisation of the human and murine genes. Brain Res Mol Brain Res 1996;35:211–9.
[30] Lynch JW, Rajendra S, Barry PH, Schofield PR. Mutations affecting the glycine receptor agonist transduction mechanism convert the competitive antagonist, picrotoxin, into an allosteric potentiator. J Biol Chem 1995;270:13799–806.
[31] Hosie AM, Akagi H, Ishida M, Shinozaki H. Actions of 3-[2′-phosphonomethyl[1,1′-biphenyl]-3-yl]alanine (PMBA) on cloned glycine receptors. Br J Pharmacol 1999;126:1230–6.
[32] Saitoh T, Ishida M, Maruyama M, Shinozaki H. A novel antagonist, phenylbenzene omega-phosphono-alpha-amino acid, for strychnine-sensitive glycine receptors in the rat spinal cord. Br J Pharmacol 1994; 113:165–70.
[33] Bræstrup C, Nielsen M, Krogsgaard-Larsen P. Glycine antagonists structurally related to 4,5,6,7-tetrahydroisoxazolo [5,4-c]pyridin-3-ol inhibit binding of [^{3}H]strychnine to rat brain membranes. J Neurochem 1986;47:691–6.
[34] Curtis DR, Malik R. Glycine antagonism by RU 5135. Eur J Pharmacol 1985;110:383–4.
[35] Simmonds MA, Turner JP. Antagonism of inhibitory amino acids by the steroid derivative RU5135. Br J Pharmacol 1985;84:631–5.
[36] LeFort D, Henke H, Cuénod M. Glycine specific [^{3}H]strychnine binding in the pigeon CNS. J Neurochem 1978;30:1287–91.
[37] Mackerer CR, Kochman RL, Shen TF, Hershenson FM. The binding of strychnine and strychnine analogs to synaptic membranes of rat brainstem and spinal cord. J Pharmacol Exp Ther 1977;201:326–31.
[38] Maksay G. Bidirectional allosteric modulation of strychnine-sensitive glycine receptors by tropeines and 5-HT_3 serotonin receptor ligands. Neuropharmacology 1998;37:1633–41.
[39] Maksay G, Laube B, Betz H. Selective blocking effects of tropisetron and atropine on recombinant glycine receptors. J Neurochem 1999;73: 802–6.